Progress In Electromagnetics Research, Vol. 144, 141–150, 2014

Synthesis of a Magnetic Field Concentrated in One Dimension

Gareth K. Sessel and Ivan W. Hofsajer*

Abstract—The focusing of a magnetic field, at low frequencies, in the very near field is difficult as flux lines naturally tend to disperse. It is not possible to use antenna array techniques due to large wavelengths at low frequencies. A method for synthesizing a concentrated magnetic field in a large air gap between two magnetic poles is presented. The focusing effect is brought about by the inclusion of side poles, adjacent to each of the main poles. Through the correct dimensioning of the side poles' reluctances and relative magneto-motive forces it is possible to focus the field in the center of the gap. General design curves for normalized parameters, determined via finite element modelling, are presented. A scale model is experimentally verified.

1. INTRODUCTION

Several applications in engineering and medicine may benefit from a low frequency magnetic field that is focusable in a large air gap between magnetic poles. The goal is to focus the magnetic flux into an area much narrower than the length of the air gap.

Focusing magnetic flux is difficult since, due to the circulatory nature of the field, it tends to disperse in order to reduce its energy density. In the very near field, where dimensions are a small fraction of a wavelength, antenna array techniques cannot be used to produce the desired effect. Furthermore, Earnshaw's theorem can be used to show that focusing a low frequency magnetic field in three dimensions is not directly attainable [1]. In order to overcome this limitation, the focusing will be performed in one dimension. This means that, along a single line that passes between the magnetic poles, the magnetic flux lines will be most concentrated at the target zone. Focusing will not occur in the other dimensions.

In the case where the air gap is large relative to the pole-width, flux fringing is responsible for the high flux densities found outside the area in-between the pole faces. Concentrating the field by means of a profiled pole does not produce good results since the profiled pole does not reduce fringing. The amount of fringing produced in an air gap between two square profile poles is shown in Fig. 1. It is well understood that flux fringing becomes more pronounced as the relative length of the air gap is increased. It can be seen that the concentration in the center of the air gap becomes very poor as the ratio of air gap-length to pole-width becomes large and there is a very significant portion of flux outside of the air gap due to fringing. The air gap can be considered to be large when the ratio of air gap-length to pole-width is large.

From the figure, it can be seen that at large air gaps (e.g., where (air gap-length)/(pole-width) = 38), the fringing is so severe that the magnitudes of the flux densities far outside of the device are similar to that in the center of the device. It is the function of the additional poles, that will be introduced adjacent to the main pole, to counteract this fringing and will be described in detail in this paper.

Some work has reported on the benefits of using a profiled magnetic field in the air gap of a linear actuator. The force density of the linear actuator is enhanced by shaping and profiling the field at the pole face using a shaded pole technique [2, 3]. Additional relevant work is [4] which makes use of a single shaped magnetic pole in a magnetic drug targeting system. This directs but does not concentrate the

Received 13 December 2013, Accepted 9 January 2014, Scheduled 14 January 2014

* Corresponding author: Ivan William Hofsajer (ivan.hofsajer@wits.ac.za).

The authors are with the School of Electrical and Information Engineering, University of Witwatersrand, South Africa.

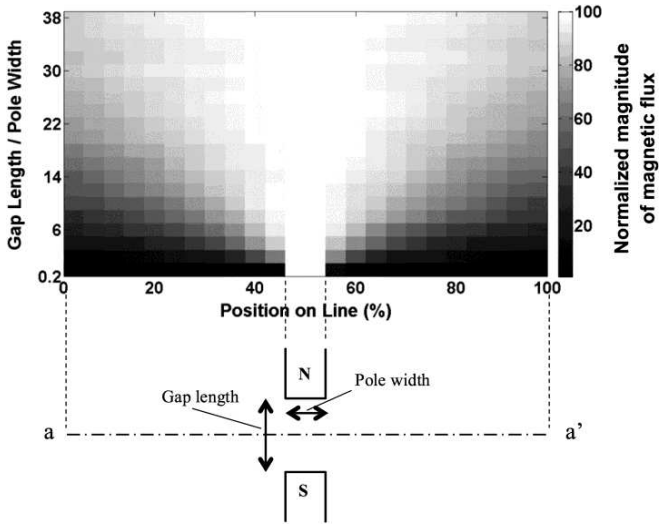

Figure 1. Normalized magnitude of fringing flux along the center line between two poles as the ratio of the air-gap length to pole-width increases.

field. Other works in the area of magnetic drug targeting use multiple coils to achieve the targeted drug delivery [1, 5].

Furthermore, the systems implementing multiple coils switch the coils using an algorithmic sequence to gradually push or pull the magnetic particles [1]. This progressively guides the medication, bound to the magnetic particles, towards the tumor region.

This paper describes a method for designing a magnetic field focusing device. The design methodology has been simplified using graphical results from multiple finite element (FEM) simulations [6]. The graphs aid in the design of any system that shares the constraints of the proposed system. The resultant apparatus is able to concentrate magnetic flux lines into an area far closer than the wavelength of the magnetic field. A small-scale physical model demonstrates that the design functions as predicted.

2. TOPOLOGY

2.1. Structure

The structure under consideration can be thought of fundamentally as an EE core with a large gap in the center leg. The core is modified in order to include several additional poles on either side of the central main pole. This is shown diagrammatically in Fig. 2. Due to the large air gap in the main pole there is appreciable fringing flux as expected. The poles on either side of the main pole carry flux in the opposite direction in an attempt to cancel out this fringing field. These poles are termed focus poles in this paper. Further focusing may be achieved by attaching additional focus pole sets to the model further away from the main pole. The four focus poles that directly neighbor the main poles will be referred to as the first set of focus poles or FP1. If four more poles are added, they are referred to as FP2 etc.. Even numbered focus poles will have flux in the same direction as the main poles and odd numbered focus poles will have flux in the opposite direction. Much of the work that follows in this paper is on maximizing the effects of these focus poles. All of the poles are attached to a common closed core around the outside to circulate the magnetic flux. Excitation coils are wound around the poles in a conventional fashion and drive magnetic flux through the poles.

It is important that the flux from each of the poles remains in the air gap to interact and does not leave a pole face and travel directly back to the common core, or leak via the side of a pole to an adjacent one. This gives rise to two basic constraints of the device. Firstly, that the pole lengths are relatively long, at least in the order of the size of the air gap. Secondly that some form of shielding

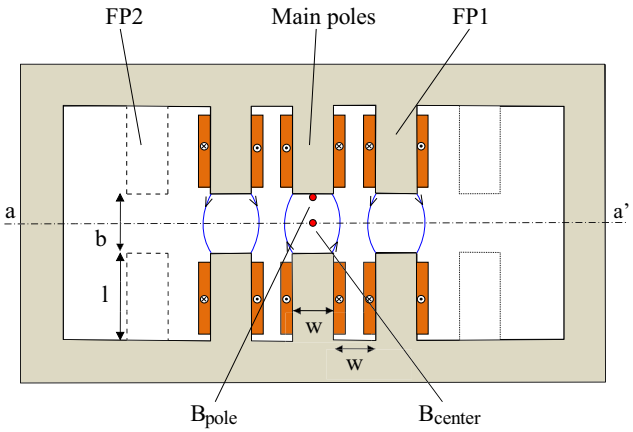

Figure 2. Structure of the focusing device.

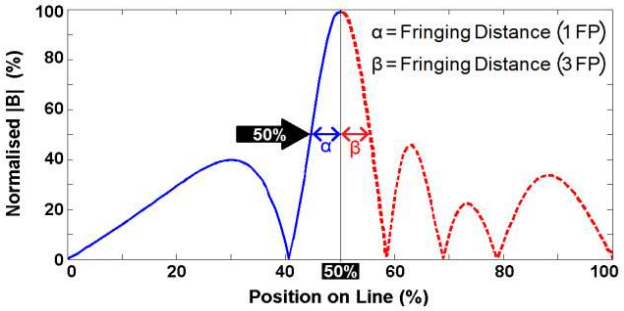

Figure 3. Typical field plot along the horizontal center line a-a' for the case of 1 (left hand side) and 3 (right hand side) focus pole sets.

is placed between the poles to prevent flux exiting at the side. This will be implemented by means of eddy current shields and are described in more detail later on.

2.2. Performance Factors

The objective of the device is to create a magnetic field peak in the center of the air gap, with the highest possible levels of attenuation on either side of that peak. In order to evaluate the effectiveness of a design, the magnetic flux density along the line a-a' in Fig. 2 is evaluated as the primary metric.

2.2.1. Fringing Distance

The fringing distance (FD) is defined as the distance along the horizontal line a-a' from the center of the line (i.e., the point along the line where the flux density is the greatest) to where the magnetic flux density has fallen to 50% of its maximum value. A typical plot of the magnetic flux density along this line is shown in Fig. 3 for the case of a single set of focus poles (solid line) and three sets of focus poles (dashed line). In order to have a comparable metric, the fringing distance is normalized to the gap length. It is a further requirement that any side lobes of the flux along the a-a' line remain below 50% of the maximum flux along the line. This requirement was strictly enforced and all FEM simulations that produced results that did not meet this requirement were discarded. Therefore, there are configurations which produce better focusing than those reported by this paper. However, these configurations have side lobes greater than this allowable limit.

2.2.2. $B_{pole} : B_{center}$

A secondary objective of the design is to achieve a suitable ratio of the amplitude of the flux at the surface of the main pole-face to the field amplitude at the center of the device. This will be defined as the $B_{pole} : B_{center}$ ratio and gives an indication of the focusing in the vertical direction. The locations of the positions of B_{pole} and B_{center} are shown in Fig. 2. Generally this ratio is large; the field at the pole face is bigger than that in the center of the device. This results in the occurrence of high field amplitudes within the air gap but outside of the focus region. It is therefore desirable to minimize the $B_{pole} : B_{center}$ ratio although this is not the primary objective.

2.3. Variable Parameters

The proposed structure results in a complex geometry. It is apparent from Fig. 2 that there are very many parameters that could be altered and which might have an impact on the two performance metrics

described above. The approach followed with the inclusion of the focus poles is to produce a flux which cancels out the fringing flux of the main pole. The same cancellation flux may be brought about by several different parameter variations. For example it may be possible to vary the excitation of a focus pole or its position. The number of variable parameters increases exponentially with additional focus pole sets.

It was found that within the fundamental geometrical constraints of the device, most parameters could be varied individually to produce the similar focusing effects. For the investigation discussed here the main two parameters that were varied to obtain the best possible performance are the focus pole lengths (thereby varying the focus pole gap-lengths) and the focus pole magneto motive forces (MMF). The focus poles' gap-lengths and MMFs were varied relative to the main focus pole gap-length and MMF respectively. These two parameters were chosen because one is based on geometry and the other is based on excitation.

The variation of these parameters is shown in Fig. 4. All other parameters were fixed. The total width of the device was constrained to be five times the air gap-length. One, two and three sets of focus-poles were considered. The distance between neighboring poles was always made equal to the pole-width. The parameters of each set of focus poles could be varied independently.

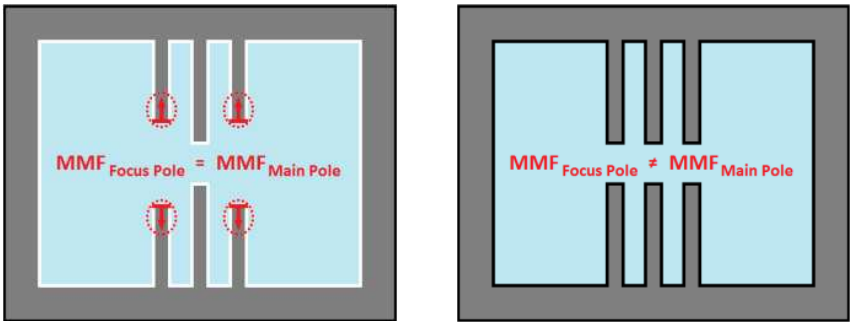

Figure 4. Parameter variations for the optimization. (a) The gap lengths of the focus poles are varied, (b) the MMF of the focus poles are varied.

In order to obtain a general solution, which can be used to design an arbitrary sized focusing device, all parameters were determined as a function of the gap-length to pole-width ratio as discussed in Section 1.

3. PERFORMANCE DATA

From the preceding section, the focus-pole MMFs and the focus-pole gap-lengths are to be optimized. The values of these parameters for each of the focus pole sets that gave the best fringing distance along the horizontal axis for a given configuration was determined via an exhaustive search using 2D FEM simulations. The FEM simulations were conducted under magneto static conditions, using ideal magnetic materials. This solution will be applicable up to several hundred kilohertz in practice provided that the eddy current losses are dealt with appropriately.

The configurations that gave the best fringing distance were recorded and the results are shown in Fig. 5 for the case of a variable focus pole MMF and Fig. 6, for the case of a variable focus-pole gap-length.

As the total inner-width (i.e., the width without the thickness of the outer frame) of the entire device was constrained to five times that of the gap length, not all solutions are possible over the full horizontal axis. The relative pole width increases as the gap-length to pole-width ratio becomes smaller. Therefore there is no longer enough space to accommodate the additional sets of focus poles. Hence the reduced amount of data towards the left side of these figures as the number of focus pole sets increases.

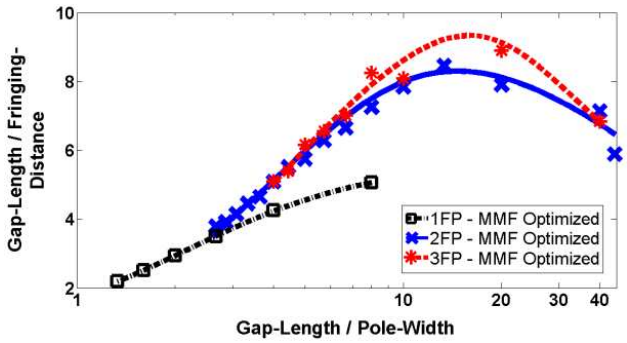

Figure 5. Fringing distance of focus pole MMF optimized device.

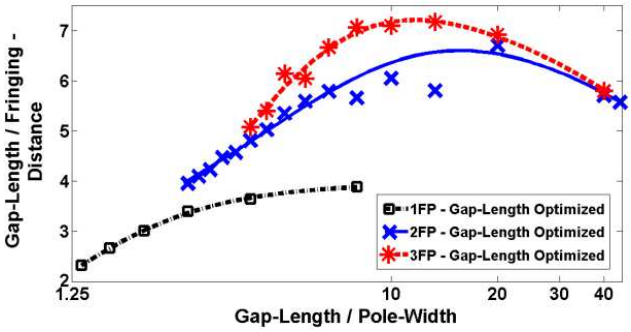

Figure 6. Fringing distance of focus pole gap-length optimized device.

In order to interpret these graphs, consider Fig. 5 where the ratio of gap-length to pole-width is 10, i.e., the gap is 10 times larger than the width of the pole. Under this condition with 2 sets of focus poles the best possible fringing distance is 1/8 of the gap length.

The fringing distance, for both the MMF and gap-length configurations, improves significantly when a second set of focus poles is added. Three focus pole sets provide some marginal improvement compared to the fringing-distance obtained using two focus pole sets. These results should be compared to Fig. 1 where it can be seen that at high values of (gap-length)/(pole-width), the field is almost uniform along the line a-a'.

Each of the configurations that leads to a point on the graphs of Figs. 5 and 6 also have a corresponding secondary performance metric: the $B_{pole} : B_{center}$ ratio. The results of this ratio for every configuration is shown in Figs. 7 and 8 for the two cases. No optimization was performed for this metric.

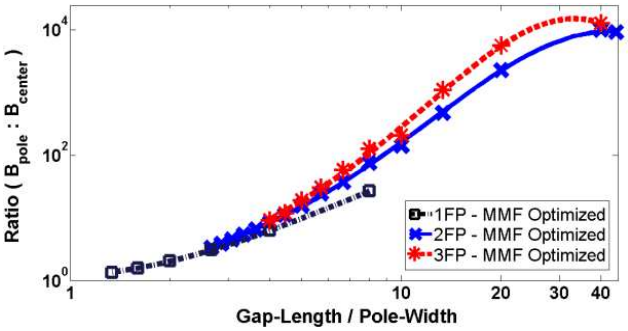

Figure 7. $B_{pole} : B_{center}$ ratio of focus pole MMF optimized device.

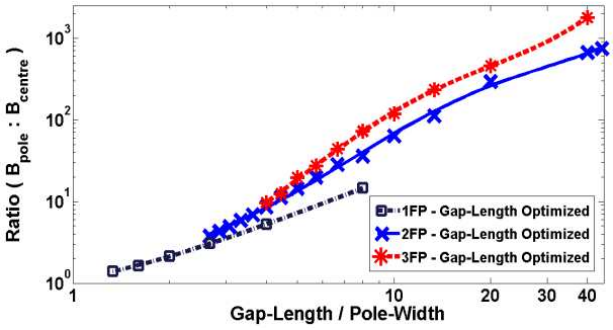

Figure 8. $B_{pole} : B_{center}$ ratio of focus pole gap-length optimized device.

There is a trade off in the focusing effects in the horizontal and vertical directions. As the fringing distance becomes smaller, the $B_{pole} : B_{center}$ ratio becomes larger. For the purposes of this investigation the fringing distance takes precedence.

From the results in these four graphs it can be seen that the focusing effect is markedly improved by increasing the number of focus poles from one set to two. However there is only a marginal increase in moving from two sets to three. The two focus pole set configuration should therefore be adopted. The slight fringing-distance improvement, in the three focus pole sets configuration, comes at the expense of a worse $B_{pole} : B_{center}$ ratio and additional system complexity and cost. At the more realistic values of gap-length/pole-width (i.e., towards the left hand side of the graphs), the benefits of the three focus pole set configuration are outweighed by its disadvantages.

4. DESIGN AND VERIFICATION

The performance curves of Fig. 5 to Fig. 8 show the best results found using the two approaches. However, these curves do not provide any information regarding the values for the focus poles' MMFs or gap-lengths in order to achieve the reported results. This information is necessary for achieving a workable design. These parameters are plotted in Figs. 14 and 15 in Appendix A as a function of (air gap length)/(pole-width). The design procedure is outlined here and was used to design an experimental prototype.

The proposed design procedure follows five steps:

1. Decide whether a gap-length controlled system or MMF controlled system is more appropriate/convenient.
2. Specify a minimum fringing distance, a maximum $B_{pole} : B_{center}$ ratio and the required main-pole gap-length for the device.
3. Using Figs. 5 and 7 for an MMF controlled system or Figs. 6 and 8 for a gap-length controlled system, find the gap-length/pole-width that satisfies, via trade-off, both the $B_{pole} : B_{center}$ requirement as well as the fringing distance requirement.
4. Using the value for gap-length/pole-width determined in step 3, along with Fig. 14 for an MMF controlled system or Fig. 15 for a gap-length controlled system, read off the values of the MMF or gap-length for each focus pole.
5. Convert the pole-widths and MMFs or gap-lengths from percentages to real values and apply to the design.

Given the information available up to this point it is not possible to determine, in absolute terms, what the actual value of the flux in the center of the device will be. This can be estimated since the ratio of the $B_{pole} : B_{center}$ value is known. The maximum field exiting the pole face can be approximated by considering the saturation flux density of the magnetic material (provided the main poles are not saturated). This in turn can be used via the ratio to determine the maximum possible flux at the center of the device. The exact absolute values of the MMF and flux density will require a FEM simulation.

The entire design procedure up to this point has been formulated using two-dimensional FEA, with the assumption of an infinitely deep model. As a result, it is important to verify the design by building a prototype and taking experimental readings.

The design of the prototype will be performed in detail, in order to serve as an example of the design procedure. The constructed device is shown in Fig. 9, with the major parameters listed in Table 1. Consider the requirements listed below.

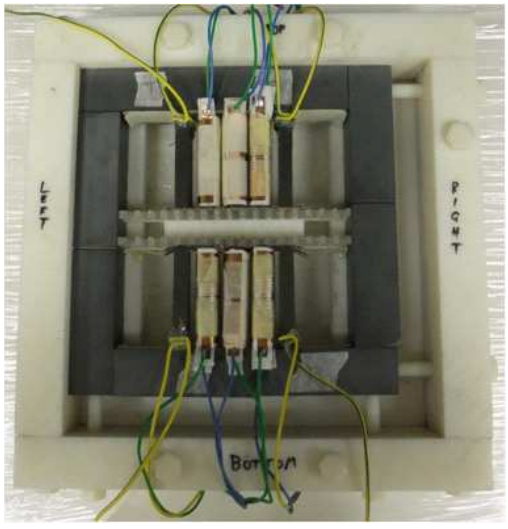

Figure 9. Experimental device.

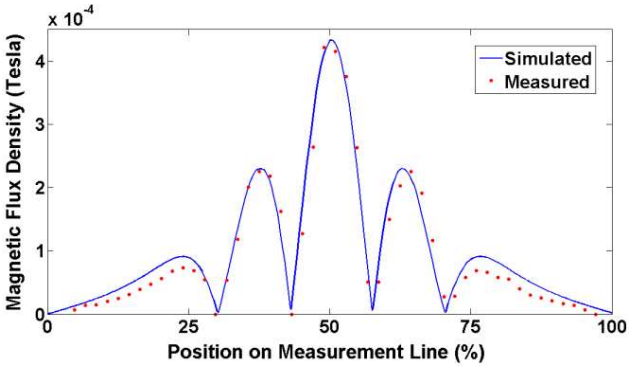

Figure 10. Performance of experimental device.

Table 1. Dimensions of various parameters of the prototype device.

	Size (mm)
Inner Core Width	157
Pole Lengths (b)	65.6
Pole Widths (w)	9
Pole-to-pole separation distances (w)	9
Air Gap Length (l)	25.8
Depth	27

A device is required to produce a focused magnetic field. The air gap-length in the central leg of the device is 25.8 mm long. The magnetic field must attenuate from its maximum in the device center to 50% of the maximum in less than 7.3 mm (along the line a-a'). Additionally, the application requires a $B_{pole} : B_{center}$ ratio less than 5 : 1. An MMF controlled system (equal gap-lengths) is specified.

The five steps from the design procedure in Section 4 will now be applied to the system in the above-mentioned example. An MMF controlled system is specified. A maximum $B_{pole} : B_{center}$ ratio of 5 : 1 and a minimum gap-length/fringing-distance of 3.53 has been stipulated (i.e., 25.8/7.3).

A two focus pole set device will be designed. Fig. 14 in the appendix contains the design curves for this type of device therefore it will be used in the design process. From Fig. 14(a), it can be seen that at a gap-length/pole-width value of 2.8, both the $B_{pole} : B_{center}$ ratio and the fringing-distance requirements are met.

Using this value of gap-length/pole-width, the MMF design curve in Fig. 14(b) can be used to determine the relative MMFs that must be applied to the focus poles in order to achieve the desired output. The inner set and outer set of focus poles must have MMFs of approximately 50% and 23% of the main pole MMF respectively.

Finally, the percentages obtained should be converted to physical dimensions so that the device can be built. A gap-length/pole-width value of 2.8 means that pole-widths (both main and focus poles) as well as the pole-to-pole separation distances should be 9 mm. Additionally, the MMFs applied to the inner set (FP1) and outer set (FP2) of focus poles should be 52% and 18% of the main pole MMF respectively. The design curves predict that this device would produce a magnetic field with a fringing-distance of approximately 6.6 mm and a $B_{pole} : B_{center}$ ratio of approximately 4.

In order to simplify the construction of the prototype device, equal current was used for all the poles. A turn ratio of 5 : 2.5 : 1 for MP : FP1 : FP2 produces a turn ratio that almost matches that specified by the design procedure. The main poles were each wrapped with 5 turns of the copper foil. The first set of focus poles were each wrapped with 3 turns of the copper foil and the second set of focus poles were each wrapped with a single turn of copper wire.

The final ratio of the MMF of the main-pole to that of the MMF of the first focus pole to that of the second focus-pole was 5 : 3 : 1.

The windings of the main pole and first set of focus poles were implemented with copper foil along the full length of the pole. These full-length windings acted as magnetic shields, since the induced eddy currents set up magnetic fields that opposed any flux lines leaking from the pole sides.

A search coil was used as the measurement sensor to determine the magnetic flux density along the middle line. The sensor was fastened to a jig designed to move the sensor into 49 equally spaced regions along the measurement line.

The measured values of flux density were overlaid on the focusing curve predicted by FEM. This is shown in Fig. 10. The measured values correspond very well with the simulated focusing pattern. This is especially true at the peaks caused by the main poles and the inner most focus poles (FP1). The maximum values of these peaks match up with the simulated values with good agreement. Additionally, the field attenuates to zero in-between peaks as predicted by the simulation.

There is a slight discrepancy between the measured and simulated values towards either end of the device, i.e., the measured values of the outermost peaks are slightly lower than expected. This can be attributed to the difference in the infinitely deep model used by the simulation and the finite thickness

of the device constructed for the experiment. Furthermore, the measured value for $B_{pole} : B_{center}$ of $4 : 1$ corresponds well with the value predicted by the FEM simulation.

5. DISCUSSION

5.1. Saturation Behavior

The design procedure ensures that the magnetic flux of the main pole set is always greater than that of the focus poles. This means that when a high output is required and the MMFs are increased, these poles will saturate first.

In both the MMF optimized system and the gap length optimized system, the second and third highest flux densities will occur in the first and second set of focus poles respectively.

The frame of the device (the return path) will generally have a low total magnetic flux density due, in part, to the local cancellation of the fluxes from the poles on each side of the device which are opposite in direction. This can be seen in Fig. 11. This means that a relatively slim frame could be used without sacrificing performance.

As saturation comes into effect, the contributions of the individual poles change. This in turn alters the focusing along the horizontal line a-a'.

If the main pole saturates, the reluctance of that flux path will increase. However, the magnetic shields will ensure that the flux will stay confined to the pole area. Due to the increased reluctance, the central peak in the magnetic field intensity along the measurement line will drop relative to the peaks caused by the focus poles. The magnetic flux density for a typical scenario in which the main poles have saturated is shown in Fig. 12.

If the relative MMFs, in either the MMF optimized system or the gap-length optimized system, are further increased to a point at which the focus poles begin to saturate, the side peaks on the measurement

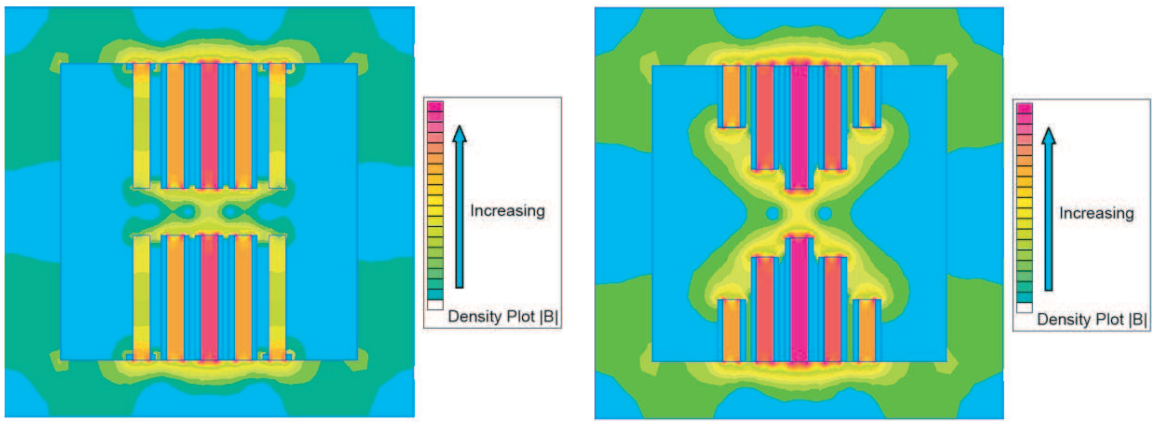

(a) (b)

Figure 11. Relative flux densities in (a) MMF optimized system and (b) gap-length optimized system. The focusing pattern can be seen in the air-gap of the device.

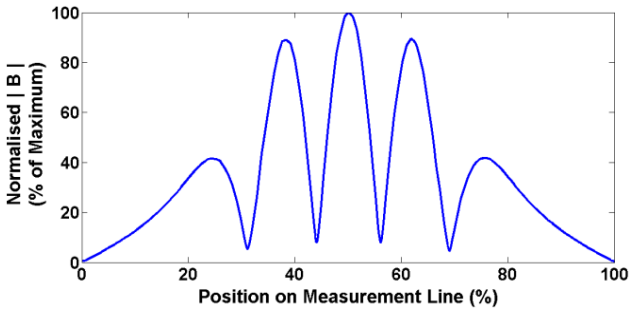

Figure 12. Focusing pattern after main pole saturates but before focusing poles begin to saturate.

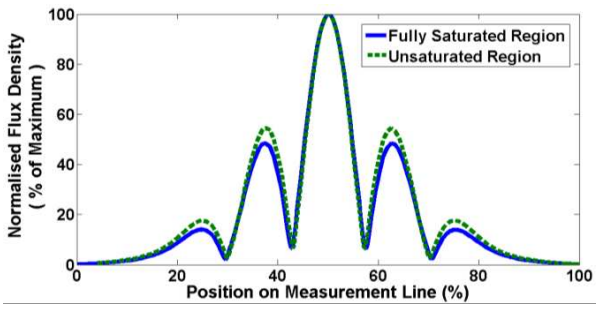

Figure 13. Plot showing similarity between the focused fields in the unsaturated and fully saturated cases.

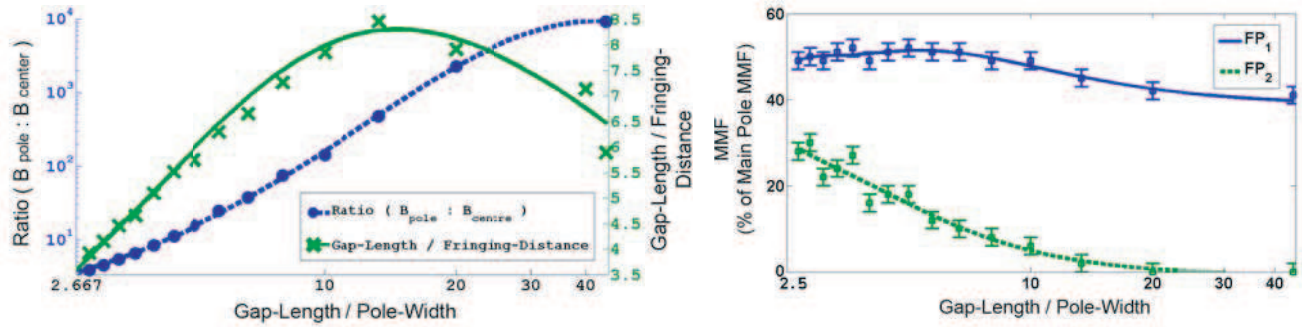

(a) (b)

Figure 14. Relative MMF design curves for two sets of focus poles.

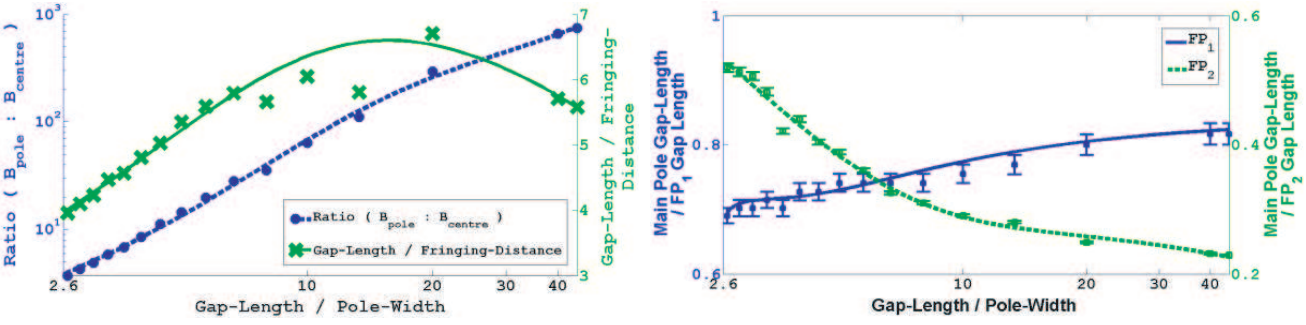

(a) (b)

Figure 15. Relative focus pole gap-length design curves for two sets of focus poles.

line will begin to decrease as well. This continues to occur until all the poles have saturated fully. At this stage, the output looks very similar in shape to the output pre-saturation, since the magnetic shields are forcing all the flux to remain it its original place. This is shown in Fig. 13.

The proposed design can be operated in different regions. In order for the peaks caused by the focus poles to remain within the pre-defined limits, the device must either be operated in the region before saturation occurs or in the region when full saturation of all the poles occurs. It is interesting to note that if operating in the saturated region, the field amplitude in the center of the device can be increased without limit whilst maintaining the focused effect, so long as sufficient MMF is available. Additionally, if operating the device in this way, it is sensible to replace the ferrite poles with air, in order to eliminate losses caused by the magnetic material.

5.2. Maximum Focusing Possibility

It becomes clear that a trade-off must be made early in the design stage. As the fringing-distance decreases, the $B_{pole} : B_{center}$ ratio increases.

Maximum focusing is directly related to the smallest fringing-distance. The largest value of gap-length/fringing-distance obtained in the investigation (i.e., the smallest fringing distance) was approximately 8.5 for a two focus pole device. In a device with a 40 cm air gap, this results in a fringing distance of approximately 4.7 cm. For a three focus pole device this number can be as high as 9.5. It is important to note that this is merely the distance taken for the field along the line a-a' to attenuate to 50% of its maximum value. 50% was chosen arbitrarily to provide a consistent method by which to compare the results of different configurations.

The details specific to another application may suggest another preferred definition for fringing-distance. For example, if the healthy tissue outside a tumor region is able to withstand a flux density of 80% of that which is required in the tumor center, then the fringing-distance could be redefined. This would result in a higher value for gap-length/fringing-distance (i.e., a smaller fringing distance) even though the device remained unchanged. It is therefore problematic to assess the performance of the device without first understanding the requirements of the specific application.

5.3. MMF vs Gap-Length Method

The MMF optimized device offers several advantages over the gap-length version. It is simpler to construct since only one size of pole is required for the construction. Additionally, varying the MMFs in real-time is far simpler than adjusting the physical lengths of the poles. This gives rise to the possibility of a device that can be adjusted in real time according to the needs of a specific application. Finally, the design curves show that the MMF optimization method produces smaller fringing-distances than the gap-length method.

However, the gap-length method produces a lower $B_{pole} : B_{center}$ ratio and it requires less excitation to achieve the same flux density at the center of the line a-a'. This is due to flux leaving one pole face and entering a neighboring pole face rather than crossing the large air-gap. The pole faces of neighboring poles are a greater distance apart in the gap-length optimized device, thereby reducing this effect. This can be seen in Fig. 11.

6. CONCLUSIONS

Focusing a low frequency magnetic field in a large air gap may prove beneficial in several applications in the engineering and medical fields. However, due to the absence of general theory regarding the production of a focused magnetic field (in the very near field), very little investigation into its use has been performed. This paper demonstrates that a low frequency magnetic field is focusable in one dimension and presents a design method to achieve specific focusing requirements. The design method incorporates the results from simulations of optimized devices, which greatly simplifies the design procedure.

For the device operating either in the fully unsaturated or fully saturated mode, the normalized design curves presented are linear and scale with arbitrary dimensions.

A prototype device was designed and built to experimentally verify the theoretical predictions. Measurements taken correspond very well with the simulated results. The device can be constructed using air poles in order to achieve an unbounded value for flux density at the center of the device, so long as there is sufficient excitation available to the device.

APPENDIX A.

Figures 14 and 15 show the curves required in order to design an arbitrary focusing device. The design procedure described in Section 4 details the use of the curves.

REFERENCES

1. Nacev, A., et al., "Towards control of magnetic fluids in patients: Directing therapeutic nanoparticles to disease locations," *IEEE Control Systems*, Vol. 32, No. 3, 32–74, 2012.
2. Dede, E. M., J. Guo, Y. Lee, L. Q. Zhou, M. Zhang, and D. Banerjee, "Kilohertz magnetic field focusing and force enhancement using metalic loop array," *Applied Physics Letters*, Vol. 101, 023506-4, 2012.
3. Lee, J., E. M. Banerjee, D. Dede, and H. Iizuka, "Magnetic force enhancement in a linear actuator by air-gap magnetic field distribution optimisation and design," *Finite Elements in Analysis and Design*, Vol. 58, 44–52, 2012.
4. Alexiou, C., et al., "A high field gradient magnet for magnetic drug targeting," *IEEE Transactions on Applied Superconductivity*, Vol. 16, No. 2, 1527–1530, June 2006.
5. Han, X., Q. Cao, and L. Li, "Design and evaluation of three-dimensional electromagnetic guide system for magnetic drug delivery," *IEEE Transactions on Applied Superconductivity*, Vol. 22, No. 3, 4401404, June 2012.
6. Sessel, G. K., "A technique for the production of a high amplitude, high frequency, concentrated magnetic field for use in hyperthermia applications," Dissertation, University of Witwatersrand, 2012.